Volume 23, No 4 | International Journal of Radiation Research, October 2025

Differentiating focal interstitial fibrosis from pulmonary adenocarcinoma in part-solid nodules using computed tomography features

D. An[1], Z. Zou[2], J. An[2], Y. Tian[2*]

[1]*Department of Medical Imaging Center, First Hospital of Qinhuangdao, Qinhuangdao, Hebei Province, China*
[2]*Department of Interventional Treatment, First Hospital of Qinhuangdao, Qinhuangdao, Hebei Province, China*

► ***Original article***

***Corresponding author:**
Ye Tian, M.D.,
E-mail: *tianye0917@163.com*

Received: November 2024
Final revised: May 2025
Accepted: July 2025

Int. J. Radiat. Res., October 2025; 23(4): 847-853

DOI: 10.61186/ijrr.23.4.3

Keywords: *Tomography, X-Ray computed; solitary pulmonary nodule; pulmonary fibrosis; adenocarcinoma of lung.*

ABSTRACT

Background: Distinguishing focal interstitial fibrosis from pulmonary adenocarcinoma based on computed tomography characteristics is challenging. We investigated the computed tomography features of part-solid lung nodules to identify characteristics useful for differentiating focal interstitial fibrosis from pre-invasive lesions or invasive pulmonary adenocarcinomas. ***Materials and Methods:*** Our research analyzed 182 part-solid lung nodules from 177 patients, comparing the computed tomography characteristics of focal interstitial fibrosis, pre-invasive lesions, and invasive pulmonary adenocarcinomas. Predictive factors for focal interstitial fibrosis were determined via binary logistic regression analysis. Predictive capability of the logistic regression model was assessed utilizing receiver operating characteristic curves. ***Results:*** Invasive pulmonary adenocarcinoma was seen in 124 part-solid lung nodules, while 21 nodules showed focal interstitial fibrosis. Binary logistic regression analysis between focal interstitial fibrosis and pre-invasive lesions revealed that irregular shape and concentrated distribution of the solid portion were significantly associated with focal interstitial fibrosis. Binary logistic regression analysis between focal interstitial fibrosis and invasive pulmonary adenocarcinomas revealed that smaller lesion size, ill-defined lesion borders, and solid portion's well-defined borders were notable independent factors linked to focal interstitial fibrosis. The model using these three predictors to distinguish focal interstitial fibrosis from invasive pulmonary adenocarcinomas achieved a high receiver operating characteristic curve area of 0.845. ***Conclusion:*** Focal interstitial fibrosis exhibited distinct computed tomography features compared to pre-invasive lesions or invasive pulmonary adenocarcinomas; the solid portion of part-solid lung nodules might serve as a valuable distinguishing feature.

INTRODUCTION

Application of computed tomography (CT) for lung cancer screening has significantly boosted pulmonary subsolid nodule detection. Subsolid nodules encompass pulmonary nodules characterized by pure ground-glass and part-solid nodules (PSNs). PSNs represent a distinct subclass of sub-solid nodules characterized morphologically by the coexistence of ground glass opacity (GGO) and solid opacity [1].

Studies have shown that PSNs possessa greater chance of being pulmonary adenocarcinomas than pure ground-glass or solid nodules [2, 3]. Pathologically, pulmonary adenocarcinomas principally comprise pre-invasive lesions and invasive pulmonary adenocarcinomas (IPAs). Pre-invasive lesions consist of atypical adenomatous hyperplasia (AAH) and adenocarcinoma in situ (AIS), whereas IPAs include minimally invasive adenocarcinoma (MIA) and invasive adenocarcinoma (IA). Accurate pathological diagnosis often necessitates invasive surgery, inevitably causing complications associated with the procedure, particularly in the case of small nodules [4]. However, PSNs often present as nonspecific radiological observations that may arise from a myriad of benign conditions, including focal interstitial fibrosis (FIF), transient inflammatory states, and hemorrhages. Although histologically benign, FIF frequently exhibits imaging characteristics that mimic those of malignant lesions, with minimal to no discernible changes evident even after prolonged radiological surveillance. Consequently, it is sometimes difficult to distinguish FIF from adenocarcinomas. In terms of treatment, FIF typically does not require invasive therapy, unlike lung adenocarcinoma [5]. Therefore, differentiating FIF from pulmonary adenocarcinomas based on initial CT data would be valuable in facilitating the development of further management strategies and reducing the need for invasive diagnostic procedures.

Previous studies have established clinical predictive models to identify benign from malignant

[DOI: 10.61186/ijrr.23.4.3]

pulmonary nodules [6-8] and pre-invasive from invasive lesions [9, 10]. Several studies have attempted to discriminate FIF from pre-invasive lesions or invasive pulmonary adenocarcinomas in PSNs, with varying results. For example, Takashima *et al.* [11] observed that FIF lesions were commonly concave and polygonal compared to lung adenocarcinoma, whereas Park *et al.* [12] reported a tendency for FIF nodules to be round or oval. Traditionally, the CT analysis of pulmonary nodules has been confined to gross morphological assessments (lesion size and margins), thereby impeding the detailed delineation of nodule features. Reports have indicated that the morphological characteristics of the solid components within nodules also offer crucial diagnostic insights [13]. Furthermore, because FIF is a component of PSNs, it is unclear whether the CT features of the solid portion of lung nodules can be used to differentiate FIF from pulmonary adenocarcinoma. Our retrospective research was designed to analyze the CT features of PSNs, particularly their solid components, to find distinguishing factors between FIF and pre-invasive lesions or invasive pulmonary adenocarcinomas. To our knowledge, this is the first research to systematically evaluate the morphological and radiological characteristics of the solid component of PSNs to identify between FIF and pre-invasive lesions or invasive pulmonary adenocarcinomas.

MATERIALS AND METHODS

Our research has got approval from the Institutional Review Board on November 11th, 2021 (approval No. 2021Q092). There was no need to get informed consent for our research, which involved reviewing the medical records and images of patients, due to its retrospective and observational nature.

Study population

Between January 2019 and June 2022, we reviewed the medical, CT, and pathological records of all patients consecutively undergoing surgical resection of pulmonary nodules at our hospital for suspected lung cancer. Inclusion in our work was determined by the following criteria: (1) the patient's clinical data were complete and available; (2) the maximum diameter of the nodule was ≤3 cm. A total of 410 nodules were collected from 388 patients. Exclusion was based on the following criteria: (1) nodules that were either purely GGO or solid; (2) pathological types other than adenocarcinoma or FIF; and (3) a previous history of pulmonary surgery or lung CT that demonstrated pulmonary nodules combined with atelectasis or pleural effusion, which may change the inherent characteristics of nodules on CT images. Ultimately, 182 PSNs from 177 patients were included in this study.

CT examinations

An unenhanced spiral acquisition chest CT was executed with a 256-slice CT scanner (Philips Healthcare, Netherlands). The CT settings included a tube voltage of 120 kVp, detector collimation ranging from 0.625 to 1.25 mm, and a beam pitch between 1.05 and 1.25. Image reconstruction was performed using full iterative reconstruction with a medium sharp algorithm and a thickness not exceeding 1.5 mm. CT scans were conducted in the supine position during full inspiration, acquiring axial images with a 1.25 mm slice thickness.

Analysis of CT features and pathological data

Two chest imaging radiologists, with 8 and 15-year working experience in thoracic CT interpretation, independently assessed all CT scans without access to pathological outcomes or clinical data. Interpretation discrepancies among the reviewers were addressed through consensus. In lung window setting (window level, −700 Hounsfield units [HU]; window width, 1500 HU), the CT features were examined utilizing a Picture Archiving and Communication System (PACS, Medi-PACS, China) workstation. Imaging analysis per lesion encompassed characteristics as below: (a) size, (b) location (upper, middle, or lower lobe), (c) shape (oval, round or irregular), (d) border (well or ill-defined), (e) lobulation, (f) spiculation, (g) bubble lucency presence, and (h) pleural indentation presence. Image features analyzed specifically for the solid component included the following: (a) proportion (≥50% or <50%), (b) distribution (scattered or concentrated), (c) location (peripheral or central), and (d) border (well or ill-defined). A round or oval lesion was defined as approximately circular. An ill-defined border was defined as the interface between nodules and surrounding lung tissue being largely unclear. Similarly, the solid portion was evaluated for having either an ill- or well-defined border at the interface with the GGO component. The solid proportion was determined using the methodology described by Lee et al. [14], which involved dividing the area of the solid portion by the total area of lesion on axial CT images. When the solid portion formed a partial boundary with the nodule, we considered the location of the solid portion to be peripheral. Otherwise, it was considered central. The scattered or concentrated distribution of the solid portion describes solid portion distribution in the entire nodule.

Histological evaluations were conducted by two experienced pathologists using conventional hematoxylin and eosin staining. The excised lung samples were immersed in 10% neutral-buffered formalin (Sigma-Aldrich, USA) for a period of 24 to 48 hours, processed using graded ethanol (Sinopharm Chemical Reagent, China) and xylene (Thermo Fisher Scientific, USA), and embedded in paraffin (Leica

[DOI: 10.61186/ijrr.23.4.3]

Paraplast, Germany). Sections measuring 4 μm were cut with a rotary microtome (Leica RM2245, Germany), mounted on slides (Citotest, China), and dried at 60 °C. Deparaffinized sections were stained with Harris hematoxylin (Baso Diagnostics, China), differentiated in acidic ethanol, stained in 0.2% ammonia water (Sigma-Aldrich), and counterstained with eosin Y (Sigma-Aldrich). After dehydration and xylene clearing, the slides were covered with neutral balsam (ZSGB-BIO, China) and imaged under a Nikon Eclipse E100 microscope (Nikon, Japan). Based on the pulmonary adenocarcinoma international multidisciplinary classification, surgical specimens were analyzed and sorted into AAH, AIS, MIA, and IA [15] .FIF is histologically characterized by interstitial septal thickening, fibroblast proliferation, and maintained intra-alveolar air space [16].

Statistical analysis

A Predictive-Probability plot was utilized to test continuous variables' normality. Continuous variables following a normal distribution were denoted as means ± standard deviation. Categorical variables were denoted as frequencies and percentages. Disparities in CT features between FIF and pre-invasive lesions or invasive pulmonary adenocarcinomas were analyzed separately. For normally-distributed continuous variables, we conducted Student's t-test, while we performed Pearson's chi-square or Fisher's exact test regarding to categorical variables. Characteristics with <0.05 p value in univariate analysis served as independent variables, and binary logistic regression analysis was employed to discover variables which might differentiate FIF from pre-invasive lesions or invasive pulmonary adenocarcinomas. As to logistic regression model, we assessed its predictive ability through the receiver operating characteristic (ROC) curve and the area under the curve (AUC). Multivariate analyses of FIF and pre-invasive lesions lacked continuous variables, and ROC curve analysis was not performed. SPSS version 25.0 (IBM, USA) for Windows was utilized to perform statistical analyses, considering p values < 0.05 as statistically significant.

RESULTS

Patient characteristics

Table 1 exhibits the demographics of 177 patients enrolled with 182 PSNs. Our study included 76 men and 101 women (average age: 58.9 ± 9.0 years); the majority (n = 121; 68.4%) had no smoking history. Eleven (6.2%) patients had a history of pulmonary or systemic malignancies. Five patients (2.8%) had two PSNs, both of which were histologically verified after a single resection. Upon thorough pathological examination of the 182 nodules in this study, the majority (n = 124; 68.1%) were found to be invasive pulmonary adenocarcinomas with subtypes of MIAs (n = 37; 29.8%) and IAs (n = 87; 70.2%). Moreover, 37 nodules (20.3%) were diagnosed as pre-invasive lesions, comprising 13 AAHs (35.1%) and 24 AIS (64.9%). The remaining 21 nodules (11.5%) were classified as FIFs.

Table 1. Clinical characteristics of enrolled patients.

Characteristics	No. of patients (n =177)
Age (years)	58.9 ± 9.0
Gender	
Male	76
Female	101
Smoking history	
Nonsmoker	121
Current or former smoker	56
Malignant history	
Present	11
Absent	166
Lesion multiplicity	
Solitary	172
Multiple	5
Number of pulmonary nodules	182
Histology	
FIF	21
AAH	13
AIS	24
MIA	37
IA	87

FIF, focal interstitial fibrosis; AAH, atypical adenomatous hyperplasia; AIS, adenocarcinoma in situ; MIA, minimally invasive adenocarcinoma; IA, invasive adenocarcinoma.

CT features of FIF and pulmonary adenocarcinoma

The CT features of FIFs and pre-invasive lesions or IPAs that appeared as PSNs are shown in table 2. Compared with pre-invasive lesions, FIFs had a more irregular shape (p = 0.009) and a more concentrated distribution in the solid portion than did pre-invasive lesions (p = 0.008, figure 1). FIFs were significantly smaller than IPAs (8.2 ± 1.7 vs. 11.4 ± 4.8 mm, p = 0.003), and were less frequently lobulated. Moreover, FIFs predominantly presented with ill-defined lesion borders of the whole nodule (p < 0.001), but a well-defined border of the solid portion (p < 0.001, figure 2). Other imaging features showed no statistical differences between FIFs and pre-invasive lesions or IPAs.

Differentiation between FIF and pulmonary adenocarcinoma

For binary logistic regression analysis between FIF and pre-invasive lesions, nodule shape and distribution of the solid portion served as input variables. The results revealed that the irregular shape and concentrated distribution of the solid portion were significantly associated with FIF (table 3). Lesion size, whole lesion border, lobulation, and border of the solid portion were utilized as input variables for binary logistic regression analysis between FIF and IPAs. Multivariate analysis identified smaller lesion size, an unclear lesion border, and a distinct border of the solid portion as

[DOI: 10.61186/ijrr.23.4.3]

significant independent factors related with FIF (table 4).

Table 2. Comparison of CT features between FIF and preinvasive lesions or IPAs.

CT features	FIF (n = 21)	Preinvasive Lesions (n = 37)	IPAs (n = 124)	FIF vs. Preinvasive Lesions	FIF vs. IPAs
				P Value	P Value
Lesion size (mm)	8.2± 1.7	8.7 ± 2.9	11.4±4.8	0.498	0.003
Location				0.384	0.301
Upper or middle lobe	10	22	74		
Lower lobe	11	15	50		
Lesion shape				0.009	0.108
Round or oval	4	20	46		
Irregular	17	17	78		
Lesion border				0.092	0.000
Well-defined	6	19	88		
Ill-defined	15	18	36		
Lobulation	4	8	64	1.00	0.006
Spiculation	2	2	35	0.615	0.069
Bubble lucency	2	4	10	1.00	0.686
Pleural indentation	6	12	34	0.760	0.913
Solid component proportion				1.00	0.279
≥50%	4	6	38		
<50%	17	31	86		
Distribution of solid portion				0.008	0.164
Scattered	2	16	30		
Concentrat-ed	19	21	94		
Location of solid portion				0.177	0.640
Peripheral	8	8	54		
Central	13	29	70		
Border of solid portion				0.437	0.000
Well-defined	13	19	30		
Ill-defined	8	18	94		

CT, computed tomography; FIF, focal interstitial fibrosis; IPAs, invasive pulmonary adenocarcinomas

Table 3. Multivariable analysis of factors differentiating between FIF and preinvasive lesions.

Variable	OR	95% CI	P Value
Irregular shape	5.778	1.500-22.261	0.011
Concentrated distribution of solid portion	8.421	1.587-44.673	0.012

FIF, focal interstitial fibrosis; OR, odds ratio; CI, confidence interval.

Table 4. Multivariable analysis of factors differentiating between FIF and IPAs.

Variable	OR	95% CI	P Value
Lesion size	0.034	0.003-0.462	0.011
Ill-defined lesion border	4.536	1.455-14.146	0.009
Well-defined border of solid portion	3.814	1.225-11.875	0.021

FIF, focal interstitial fibrosis; IPAs, invasive pulmonary adenocarcinomas; OR, odds ratio; CI, confidence interval.

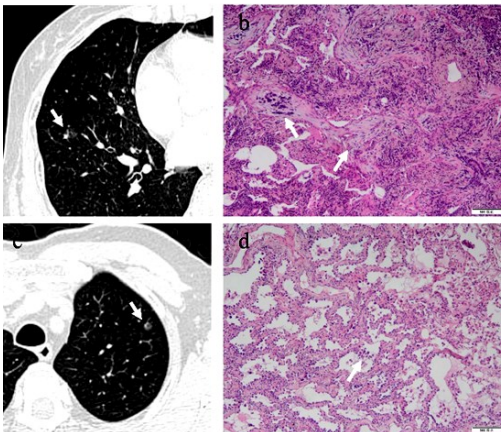

Figure 1. A 59-year-old female patient with a PSN (white arrow) in the lower lobe of the right lung. **(a)** Axial CT image revealed an 8-mm nodule with an irregular shape and concentrated distribution of the solid portion. **(b)** Microscopic photographs reveal fibrous interstitial proliferation (white arrow) accompanied by inflammatory cell infiltration. The pathological diagnosis was FIF (hematoxylin–eosin, 100×). A 69-year-old male patient with a PSN (white arrow) in the upper lobe of the left lung. **(c)** Axial CT image showing a 6-mm nodule with a regular shape and scattered distribution of the solid portion. **(d)** Microscopic photographs showing pure tumor cells growing strictly adherent to the wall (white arrow) without stromal or vascular infiltration. The pathological diagnosis was AIS (hematoxylin–eosin, 100×).

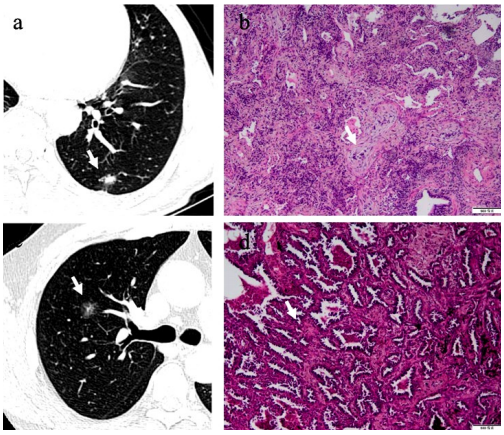

Figure 2. A 42-year-old female patient with a PSN (white arrow) in the lower lobe of her left lung. **(a)** Axial CT image revealed a 10-mm nodule with an ill-defined lesion border and a well-defined border of the solid portion. **(b)** Microscopic photographs reveal fibrous interstitial proliferation (white arrow) accompanied by inflammatory cell infiltration. The pathological diagnosis was FIF (hematoxylin–eosin, 100×). A 60-year-old male patient with a PSN (white arrow) in the upper lobe of the right lung. **(c)** Axial CT image showing a 12-mm nodule with a well-defined lesion border and an ill-defined border of the solid portion. **(d)** Microscopic photographs reveal the invasion of malignant glands into the fibrous stroma (white arrow). The pathological diagnosis was IA (hematoxylin–eosin, 100×).

ROC curve analysis assessed the logistic regression model's ability to differentiate FIF from IPAs, yielding an AUC of 0.845 (95% confidence interval: 0.750–0.940, $p < 0.001$). Compared to lesion

[DOI: 10.61186/ijrr.23.4.3]

size alone, this predictive model exhibited enhanced discriminative power (figure 3).

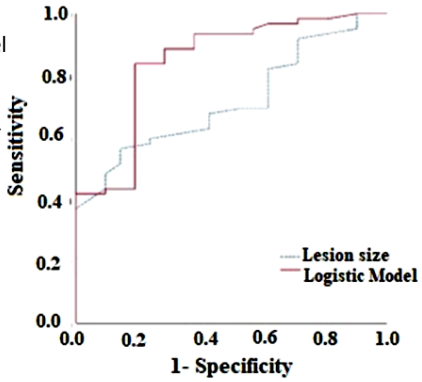

Figure 3. The AUC of the logistic model generated with lesion size, lesion border, and border of the solid portion is higher (AUC=0.845; 95% CI: 0.750-0.940) than the AUC of lesion size alone in distinguishing FIF from IPAs.

DISCUSSION

Most PSNs have been confirmed to be pulmonary adenocarcinomas. However, the incidence of FIF has increased with increased screening and pathological diagnosis of lung nodules. FIF has CT features similar to those of pulmonary adenocarcinomas, making differentiation challenging. Therefore, differentiating FIF from pulmonary adenocarcinomas based on CT features is important to reduce unnecessary invasive diagnostic procedures. The present study analyzed the CT features of FIF and both pre-invasive lesions and IPAs, with a special emphasis on the solid portion. The irregular shape and concentrated distribution of the solid portion were strongly linked to FIF compared to pre-invasive lesions. Compared to IPAs, significant independent factors related to FIF included smaller lesion size, ill-defined lesion borders, and well-defined borders of the solid portion. This study formulated a predictive model for PSNs that could differentiate between FIF and IPAs.

Previously published reports have investigated the differentiation of FIF from pulmonary adenocarcinoma based on imaging features. Si *et al.* [16] reported that a concave margin was confirmed in a high proportion of FIFs and could be used to distinguish FIFs from malignant or premalignant GGO nodules. Park *et al.* [12] described thin-section CT features of FIF in nine patients and found that more than half of the FIFs had a round or oval shape and smooth lesion margins. Ko *et al.* [17] showed that a well-defined nodule border, nodule thickness of >4.2 mm, and coronal/axial ratio of >0.62 were associated with malignancy. Geng *et al.* [18] developed a radiomics model focused on solid lung tumors, and the predictive ability of the radiomics model for differentiating lung adenocarcinoma from granuloma was significantly enhanced by the features of the 5-mm peritumoral area around solid lung tumors. Despite some differences between these studies, some results of the current study conform to those of previous reports. Notably, this study compared the CT features of FIF with those of pre-invasive lesions and IPAs and analyzed the differences between groups in the most critical aspect, the solid portion of the PSNs, as emphasized in previous publications.

According to the Fleischner Society's guidelines, nodule size is crucial for differentiating benign from malignant subsolid nodules [19]. Several studies have confirmed the higher likelihood of malignancy in larger nodules [7, 20, 21]. However, different studies have presented different perspectives on the correlation between nodule size and risk of malignancy. Some studies have found that, while larger nodules may be more likely to be diagnosed as malignant in certain cases, this does not necessarily imply that smaller nodules are inherently benign. Some small nodules may also carry a high risk of malignancy, particularly when exhibiting other suspicious characteristics [22]. In this study, IPAs' size was significantly larger compared with FIFs, again confirming that nodule size helped distinguish FIF from IPAs. However, a statistically significant disparity was found between the size of FIF and pre-invasive lesions. Due to the low probability of tumor growth, benign and pre-invasive PSNs typically have small lesions.

The CT features of the lesion shape and border provide significant diagnostic value for differentiation. However, the results vary across studies. One piece of research indicated that progressive lesions tend to manifest as round or oval shapes with clear margins, along with tracheal signs, vascular changes, and pleural alterations [23]. Research also suggested that characteristics such as spiculation, lobulation, pleural indentation, irregular forms, and indistinct edges were more prevalent [24]. In this study, marked differences in lesion shape and border features were observed between FIF and both pre-invasive lesions and IPAs. In the present study, well-defined IPA borders' frequency was dramatically higher compared with FIF. The characteristics of the lung nodule borders align with prior studies indicating that nodules with clear borders are more possibly to be malignant tumors [25]. Pathologically, although cancer cells infiltrate the surrounding tissue, this infiltration is inhibited by the interlobular septa, resulting in well-defined borders. Conversely, gradually decreasing inflammation in the surrounding tissues may be associated with ill-defined FIF borders. Compared to pre-invasive lesions, FIFs were more likely to have an irregular shape. FIFs are characterized by stromal fibers and dense inflammatory cells, and contraction of these fibers contributes to their irregular shape. Most pre-invasive lesions result from lepidic growth patterns along the alveolar lining without destruction of the alveolar wall and appear round or oval. IPAs are also prone to irregular shapes owing to minimal invasion of the stroma [26], resulting in no significant differences from FIFs in terms of nodule shape. The

[DOI: 10.61186/ijrr.23.4.3]

combination of malignant infiltration and fibroblast proliferation results in nodular lobulation, which is more common in IPAs. However, fibroblast proliferation is common to both FIFs and adenocarcinomas. In the univariate analysis, lobulation was significantly less frequent in FIF than in IPAs, but it did not hold significance in the multivariate analysis.

The solid portion is the most critical component of PSNs, and careful evaluation often provides additional evidence to differentiate FIF from pulmonary adenocarcinoma. Previous studies have principally focused on the differences in the solid portions when comparing benign and malignant subsolid nodules [7], or between various subtypes of pulmonary adenocarcinoma [27]. Li *et al*. [13] found that PSNs with irregular and scattered solid components had a high likelihood of being malignant. Gong *et al*. compared the CT features of minimally invasive and invasive adenocarcinomas. The results showed that nodules with a solid component ratio of ≥20.96% were more likely to be invasive adenocarcinomas, and that the high-risk pathological type of lung adenocarcinoma was related to the solid component ratio. A solid component ratio of 69.536% or higher suggested a greater likelihood of the nodule being a high-risk pathological type of lung adenocarcinoma [28]. However, differences in the solid portion between FIF and pre-invasive lesions or IPAs have not been well studied. Studies that focused on the solid components of FIF compared to pre-invasive lesions or IPAs showed that a concentrated distribution of the solid portion was significantly associated with FIF compared to pre-invasive lesions. Additionally, a well-defined border of the solid portion was notably linked to FIF compared with IPAs. In the current research, solid components' characteristics were combined with the overall characteristics of the nodules to provide a more comprehensive method for distinguishing FIF from pulmonary adenocarcinomas.

This study has some limitations. First, the pathological findings were gathered from patients who had surgical removal, which was driven considerably by the need for pathological assurance to avoid overlooking a malignancy. As a result, the number of FIF patients in our research was limited, which possibly had caused selection bias. Second, this study was restricted to comparing the CT features of FIF with those of pulmonary adenocarcinoma and may not apply to other benign pulmonary nodules, such as focal pneumonia or alveolar hemorrhage. Third, a notable limitation of this research was the failure to quantitatively assess the CT features.

In conclusion, FIF can be accurately distinguished from pulmonary adenocarcinomas by analyzing the CT features of PSNs. Specifically, FIF can be identified from pre-invasive lesions through its irregular shape and concentrated distribution in the solid portion. Smaller lesion size, ill-defined lesion borders, and well-defined borders of the solid portion are characteristics of FIF that differentiate it from IPAs.

***Acknowledgements*:** Not applicable.
***Funding*:** This study was upheld by the Qinhuangdao Science-Technology Support Project of China (202101A205).
***Conflicts of Interest*:** All authors declare no conflicts of interest.
***Ethical considerations*:** This single-center retrospective study was approved by the Institutional Review Board on November 11th, 2021 (approval No. 2021Q092) to review medical records and images of each patient were reviewed.
***Author contributions*:** Study conception and design: DY A, ZB Z, and Y T; data collection: all authors; analysis and interpretation of the data: JL A and Y T; statistical analysis: DY A and Y T; drafting of the manuscript: DY A; critical revision of the manuscript: JL A, ZB Z, DY A, and Y T.
***Declaration of AI usage*:** All authors declare that they didn't utilize generative AI tools while preparing this manuscript. All content, including text, data analysis, and conclusions, was produced solely by the human authors.

REFERENCES

1. He X, Li X, Wu Y, *et al.* (2022) Differential diagnosis of nonabsorbable inflammatory and malignant subsolid nodules with a solid component ≤5 mm. *Journal of Inflammation Research,* ***15:*** *1785-1796.*
2. Lee H, Goo J, Lee C, *et al.* (2007) Nodular ground-glass opacities on thin-section CT: size change during follow-up and pathological results. *Korean Journal of Radiology,* ***8:*** *22-31.*
3. Henschke C, Yankelevitz D, Mirtcheva R, *et al.* (2002) CT screening for lung cancer: frequency and significance of part-solid and nonsolid nodules. *American Journal of Roentgenology,* ***178:*** *1053-1057.*
4. Smyth R and Billatos E (2024) Novel strategies for lung cancer interventional diagnostics. *J Clin Med,* ***13****: 7207.*
5. Woo JH, Kim JH, Jeong DY, *et al.* (2024) Differentiation between invasive adenocarcinoma and focal interstitial fibrosis among persistent pulmonary part-solid nodules: with emphasis on the CT morphologic analysis. *Journal of Thoracic Imaging,* ***39:*** *335-341.*
6. Chen X and Xu B (2022) Application of CT postprocessing reconstruction technique in differential diagnosis of benign and malignant solitary pulmonary nodules and analysis of risk factors. *Computational and Mathematical Methods in Medicine,* ***2022:*** *9739047.*
7. Yang W, Sun Y, Fang W, *et al.* (2018) High-resolution computed tomography features distinguishing benign and malignant lesions manifesting as persistent solitary subsolid nodules. *Clinical Lung Cancer,* ***19:*** *e75-e83.*
8. Duan L, Shan W, Guo L, *et al.* (2022) Correlation in high resolution computed tomography signs with pathological subtype and differentiation degree of lung adenocarcinoma. *International Journal of Radiation Research,* ***20:*** *679-685.*
9. Qi L, Lu W, Yang L, *et al.* (2019) Qualitative and quantitative imaging features of pulmonary subsolid nodules: differentiating invasive adenocarcinoma from minimally invasive adenocarcinoma and preinvasive lesions. *Journal of Thoracic Disease,* ***11:*** *4835-4846.*
10. Chae H, Park C, Park S, *et al.* (2014) Computerized texture analysis of persistent part-solid ground-glass nodules: differentiation of preinvasive lesions from invasive pulmonary adenocarcinomas. *Radiology,* ***273:*** *285-293.*

[DOI: 10.61186/ijrr.23.4.3]

11. Takashima S, Sone S, Li F*, et al.* (2003) Small solitary pulmonary nodules (< or =1 cm) detected at population-based CT screening for lung cancer: Reliable high-resolution CT features of benign lesions. *Am J Roentgenol,* ***180:*** *955-964.*
12. Park CM, Goo JM, Lee HJ*, et al.* (2007) Focal interstitial fibrosis manifesting as nodular ground-glass opacity: thin-section CT findings. *Eur Radiol,* ***17:*** *2325-2331.*
13. Li W J, Lv F J, Tan Y W*, et al.* (2022) Benign and malignant pulmonary part-solid nodules: differentiation via thin-section computed tomography. *Quant Imaging Med Surg,* ***12:*** *699-710.*
14. Lee S M, Park C M, Goo J M*, et al.* (2013) Invasive pulmonary adenocarcinomas versus preinvasive lesions appearing as ground-glass nodules: differentiation by using CT features. *Radiology,* ***268:*** *265-273.*
15. Travis W, Brambilla E, Noguchi M*, et al.* (2011) International association for the study of lung cancer/american thoracic society/ european respiratory society international multidisciplinary classification of lung adenocarcinoma. *Journal of Thoracic Oncology,* ***6:*** *244-285.*
16. Si M, Tao X, Du G*, et al.* (2016) Thin-section computed tomography-histopathologic comparisons of pulmonary focal interstitial fibrosis, atypical adenomatous hyperplasia, adenocarcinoma in situ, and minimally invasive adenocarcinoma with pure ground-glass opacity. *European Journal of Radiology,* ***85:*** *1708-1715.*
17. Ko K-H, Huang T-W, Chang W-C*, et al.* (2021) Differentiating focal interstitial fibrosis from adenocarcinoma in persistent pulmonary subsolid nodules (> 5 mm and < 20 mm): the role of coronal thin-section CT images. *European Radiology,* ***31:*** *8326-8334.*
18. Geng Y, Sun L, Sun M*, et al.* (2022) The significance of peritumoral 5mm regions features for radiomics model in distinguishing the lung adenocarcinomas and granulomas. *International Journal of Radiation Research,* ***20:*** *737-745.*
19. MacMahon H, Naidich D, Goo J*, et al.* (2017) Guidelines for management of incidental pulmonary nodules detected on CT images: From the fleischner society 2017. *Radiology,* ***284:*** *228-243.*
20. Eguchi T, Yoshizawa A, Kawakami S*, et al.* (2014) Tumor size and computed tomography attenuation of pulmonary pure ground-glass nodules are useful for predicting pathological invasiveness. *PloS one,* ***9:*** *e97867.*
21. Snoeckx A, Reyntiens P, Desbuquoit D*, et al.* (2018) Evaluation of the solitary pulmonary nodule: size matters, but do not ignore the power of morphology. *Insights into Imaging,* ***9:*** *73-86.*
22. Bo Y H, Ahn H Y, Lee Y H*, et al.* (2011) Malignancy rate in sonographically suspicious thyroid nodules of less than a centimeter in size does not decrease with decreasing size. *Journal of Korean Medical Science,* ***26:*** *237-242.*
23. Qi L, Xue K, Li C*, et al.* (2019) Analysis of CT morphologic features and attenuation for differentiating among transient lesions, atypical adenomatous hyperplasia, adenocarcinoma in situ, minimally invasive and invasive adenocarcinoma presenting as pure ground-glass nodules. *Sci Rep,* ***9:*** *14586.*
24. Wu H, Zhang X, Zhong Z (2025) Exploration of CT-based discrimination and diagnosis of various pathological types of ground glass nodules in the lungs. *BMC Med. Imaging,* ***25:*** *119.*
25. Gao F, Sun Y, Zhang G*, et al.* (2019) CT characterization of different pathological types of subcentimeter pulmonary ground-glass nodular lesions. *The British Journal of Radiology,* ***92:*** *20180204.*
26. Park C, Goo J, Lee H*, et al.* (2007) Nodular ground-glass opacity at thin-section CT: histologic correlation and evaluation of change at follow-up. *Radiographics,* ***27:*** *391-408.*
27. Wang H, Weng Q, Hui J*, et al.* (2020) Value of TSCT features for differentiating preinvasive and minimally invasive adenocarcinoma from invasive adenocarcinoma presenting as subsolid nodules smaller than 3 cm. *Academic Radiology,* ***27:*** *395-403.*
28. Gong X and Huang C (2024) Clinical value of CT imaging features to predict infiltration degree and pathological subtype of ground glass lung adenocarcinoma. *International Journal of Radiation Research,* ***22:*** *909-918.*

[DOI: 10.61186/ijrr.23.4.3]